SPECTROSCOPIC PROPERTIES INCLUDING LINE STRENGTHS, WAVELENGTHS, AND TRANSITION PROBABILITIES FOR Hf LXII**

G. G. Konan

Department of Physics, Science Faculty, Sakarya University, Sakarya, Turkey;
e-mail: ggunday@sakarya.edu.tr

The main focus of this study is the spectroscopic properties of highly charged hafnium ions. Highly charged ions of high-Z elements (Z ~ 70–83) are of great importance in atomic physics, astronomical physics and especially plasma diagnostics. Therefore, we perform level energies, transition probabilities, wavelengths, and line strengths for electric dipole, electric quadrupole, and magnetic dipole transitions in Hf LXII (Hf^{61+}, Z = 72). All values are calculated using the AUTOSTRUCTURE atomic structure code whose relativistic corrections are introduced according to the Breit–Pauli distorted wave approach. Valence–valence, core–valence and core–core electron correlation effects are included. The results are compared with other studies from the National Institute of Standards and Technology database. The present results are in good agreement with other studies in the literature. We hope to fill a lack of atomic data for highly charged hafnium ions, which may be useful in plasma diagnostics.

Keywords: *energies, transition probabilities, wavelengths, line strengths.*

СПЕКТРОСКОПИЧЕСКИЕ ХАРАКТЕРИСТИКИ ДЛЯ Hf LXII: СИЛА ОСЦИЛЛЯТОРА, ДЛИНЫ ВОЛН И ВЕРОЯТНОСТИ ПЕРЕХОДОВ

G. G. Konan

УДК 543.42

Университет Сакарья, Сакарья, Турция; e-mail: ggunday@sakarya.edu.tr

(Поступила 6 сентября 2022)

Изучены спектроскопические свойства высокозарядных ионов гафния. Определены энергии уровней, вероятности переходов, длины волн и силы осцилляторов для электрических дипольных, электрических квадрупольных и магнитных дипольных переходов в Hf LXII (Hf^{61+}, Z = 72) с использованием кода атомной структуры AUTOSTRUCTURE, релятивистские поправки которого вводятся в соответствии с подходом искаженных волн Брейта–Паули. Учтены эффекты корреляции электронов валентность-валентность, ядро-валентность и ядро-ядро. Полученные результаты хорошо согласуются с известными данными из базы данных Национального института стандартов и технологий.

Ключевые слова: *энергии, вероятности перехода, длины волн, силы линий.*

Introduction. Highly charged ions of atoms in the 6th row of the periodic table (*Z* = 70–83) are very important for atomic physics, astronomical physics and other research like fusion applications – for example, tungsten (*Z* = 74) is used as a plasma-facing material in tokamaks, such as ITER (International Thermonuclear Experimental Reactor) [1], while gold ions are important for plasma science, fusion reaction, biomedical applications, and high-energy astrophysics [2]. Mercury (*Z* = 80) and its ions are used in spectral sources and continuous wave and pulsed mercury lasers [3].

Thus, high-precision atomic data are required for the interpretation of spectra of highly charged heavy elements; therefore, we have performed a comprehensive investigation of spectral properties for highly

** Full text is published in JAS V. 90, No. 4 (http://springer.com/journal/10812) and in electronic version of ZhPS V. 90, No. 4 (http://www.elibrary.ru/title_about.asp?id=7318; sales@elibrary.ru).

charged heavy elements like tungsten, gold, bismuth, mercury [4–7] over the last few years. Highly charged heavy elements in the 6th row of the periodic table need to be investigated further. We continue our investigation with hafnium ions ($Z = 72$), which are created from a transmutation of tungsten induced by neutron irradiation during the operational period of the ITER reactor [8]. The National Institute of Standards and Technology (NIST) Atomic Spectra Database [9] provides only a little data for spectroscopic properties of hafnium ions.

We present energies, transition probabilities, wavelengths, and line strengths for electric dipole (E1), electric quadrupole (E2), and magnetic dipole (M1) transitions in Na-like Hf LXII (Hf^{61+}, $Z = 72$). Also, Na-like orbital spectrum is of interest for L-layer diagnosis of very high temperature laboratory plasmas such as ITER [10]. There is no comprehensive data about sodium-like hafnium ions in the literature. Early calculations were reported [11–16], but there have been only a few studies in the last 10 years. Gillaspy et al. presented the $D1$ ($3s$–$3p_{1/2}$) and $D2$ ($3s$–$3p_{3/2}$) transitions in Na-like ions [17, 18], while Sapirstein and Cheng calculated energy levels of sodium-like hafnium [19]. Energy levels for Na-like ions including Na-like Hf were performed by Fontes and Zhang [20].

The aim of the present paper is to provide an extended accurate data set of energy levels, wavelengths, transition probabilities, and line strengths for E1, E2, and M1 transitions in Na-like Hf LXII. The paper is organized as follows.

Calculation method. Calculations were done by using AUTOSTRUCTURE code developed by Badnell [21, 22] to study energy levels and radiative properties. In this code, the configuration set is chosen optionally and there is an additional new configuration to improve accuracy (a configuration interaction expansion, CI expansion). The CI expansion is related to the choice of radial functions. Each (nl) radial function is calculated in the Thomas–Fermi or the Slater-type-orbital potential model. The Hamiltonian in any coupling model (LS, IC, or ICR) is diagonalized to obtain eigenvalues and eigenvectors with which to construct the rates. Detailed information on the method of this code can be found in [21–23] of which the following is a brief summary.

Wave functions are calculated with the Breit–Pauli relativistic corrections. This Hamiltonian can be written as

$$H_{\mathrm{BP}} = H_{\mathrm{NR}} + H_{\mathrm{RC}}, \tag{1}$$

where H_{NR} is the usual nonrelativistic Hamiltonian

$$H_{\mathrm{NR}} = \sum_{i=1}^{N} h(i) + \sum_{j>i=1}^{N} \frac{1}{r_{ij}} = \sum_{i=1}^{N}\left(-\frac{1}{2}\nabla_i^2 - \frac{Z}{r_i}\right) + \sum_{j>i=1}^{N} \frac{1}{r_{ij}} \tag{2}$$

and H_{RC} contains the relativistic correction operators which include one-body relativistic operators (the spin-orbit interaction, the non-fine-structure mass variation, and the one-body Darwin corrections) and two-body Breit operators (spin-other-orbit, the mutual spin-spin, the spin-spin contact, the two body Darwin and the orbit-orbit terms).

Results and discussion. In this study, the energy levels and transition parameters for E1, E2, and M1 transitions for highly ionized hafnium ion (Hf LXII, Hf^{61+}, $Z = 72$) have been reported. In this section, we discuss the accuracy and reliability of the data through tables and graphics. We have also calculated the root mean square (RMS) value of the relative differences. The following relations are used to calculate the RMS of relative difference (r_d):

$$\%\ \mathrm{RMS} = \sqrt{\frac{1}{N}\sum(r_{d1}^2 + r_{d2}^2 + \ldots + r_{dN}^2)}\ . \tag{3}$$

In the present calculations, we have taken into account the configurations: nl ($n = 3$–6, $l = 0$–5), $2p^5 3snl$ ($n = 3$–5, $l = 0$–4), $2p^5 3pnl$ ($n = 3$–5, $l = 0$–4), $2p^5 3dnl$ ($n = 3$–5, $l = 0$–4), $2p^4 3s^2 3p$, $2p^4 3s^2 3d$, $2s2p^5 3s^2 3p$. The values of energy levels for the low-lying 32 states are listed and compared with the other studies in Table 1. Also, the percentage of relative differences between the present energies and other results [12, 14–16] is plotted in Fig. 1, whereby the comparison shows that the present energies are in good agreement. Some energy values reported with the other studies are converted to cm^{-1} in order to simplify the comparison with our values. The RMS of the relative difference are 0.6, 0.7, 0.6, 0.4, and 0.5% from references [20, 12, 14–16], respectively. Figure 1 and the RMS of the relative difference confirm our energy results' reliability and display sufficient accuracy. There are no other data sets available for comparison for higher levels.

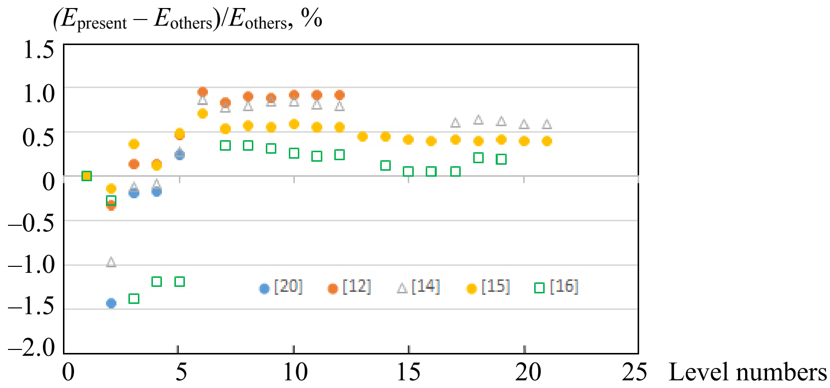

Fig. 1. The percentage of relative differences between the present energies and other results [12, 14–16, 20].

TABLE 1. Energies (E) for Low Lying Level of Hf^{61+}

Index	Levels		E, cm^{-1}	
	Conf.	Term	This work	Other works
1	3*s*	$^2S_{1/2}$	0	0
2	3*p*	$^2P_{1/2}$	1221839	1239592[a], 1233059[b], 1233268.2[c],1233319.4[d], 1233778[e], 1225890[f] 1233452[g] 1233761[h], 1223542[i],1225120[k]
3	3*p*	$^2P_{3/2}$	3877638	3884686[a], 3880089[b], 3880149.8[c], 3880631.8[d], 3880537[e], 3872153 [f] 3880258 [g] 3881988[h],3863393[i], 3931560[k]
4	3*d*	$^2D_{3/2}$	5338489	5347291[a],5331138[f], 5342900 [h],5332128[i],5402350[k]
5	3*d*	$^2D_{5/2}$	5963888	5949061[a], 5935554[f], 5947080[h],5934624[i],6035120[k]
6	4*s*	$^2S_{1/2}$	24765500	24531714[f], 24551000[h], 24591831[i]
7	4*p*	$^2P_{1/2}$	25245806	25037452[f], 25050100[h], 25108026[i], 25158530[k]
8	4*p*	$^2P_{3/2}$	26355156	26120693[f], 26143800[h], 26204939[i], 26264400 [k]
9	4*d*	$^2D_{3/2}$	26912556	26674172[f], 26685500[h], 26761461[i], 26829610[k]
10	4*d*	$^2D_{5/2}$	27185632	26935482[f] ,26955400[h], 27027624[i], 27114110 [k]
11	4*f*	$^2F_{5/2}$	27478146	27225744[f], 27253000[h], 27326049[i], 27413020 [k]
12	4*f*	$^2F_{7/2}$	27594181	27340384[f], 27374000[h], 27438967[i], 27528390[k]
13	5*s*	$^2S_{1/2}$	35693009	35528753[i]
14	5*p*	$^2P_{1/2}$	35951690	35786800[i], 35908570[k]
15	5*p*	$^2P_{3/2}$	36498534	36343323[i], 36479810[k]
16	5*d*	$^2D_{3/2}$	36765818	36617551[i], 36742260[k]
17	5*d*	$^2D_{5/2}$	36906266	36684000[h], 36754665[i], 36885390[k]
18	5*f*	$^2F_{5/2}$	37050106	36815000[h], 36899845[i], 36974280[k]
19	5*f*	$^2F_{7/2}$	37109993	36880000[h], 36956304[i], 37034390[k]
20	5*g*	$^2G_{7/2}$	37129641	36908000[h], 36980500[i]
21	5*g*	$^2G_{9/2}$	37164887	36949000[h], 37012763[i]
22	6*s*	$^2S_{1/2}$	41928683	–
23	6*p*	$^2P_{1/2}$	42086572	–
24	6*p*	$^2P_{3/2}$	42392833	–
25	6*d*	$^2D_{3/2}$	42540349	–
26	6*d*	$^2D_{5/2}$	42621342	–
27	6*f*	$^2F_{5/2}$	42702383	–
28	6*f*	$^2F_{7/2}$	42737463	–
29	6*g*	$^2G_{7/2}$	42749786	–
30	6*g*	$^2G_{9/2}$	42770237	–
31	6*h*	$^2H_{9/2}$	42770769	–
32	6*h*	$^2H_{11/2}$	42784318	–

[a,b,c,d,e,f,g,h,i,k] Ref. [20, 19, 18, 17, 11, 12, 13, 14, 15, 16], respectively.

Table 2 lists the comparison of the wavelengths (λ), transition probabilities (A_{ij}), and line strengths (S) for electric dipole (E1) transitions among states with principal quantum numbers $n = 3$ and 4. Figure 2a displays the relation of the line strengths values between this work (S_{TW}) and other works (S_{OW}) [12]. We have instead compared the transition line strengths S because the latter parameters do not explicitly depend on the transition energy. As can be seen from Table 2 and Fig. 2a, the wavelengths, transition probabilities, and line strengths are quite close to the theoretical data of the other studies [11, 12, 14, 17].

We have calculated wavelengths (λ, in Å), transition probabilities (A_{ij}, in s^{-1}), and line strengths (S, in a. u.) for electric dipole (E1) transitions among the principal quantum numbers $n = 5$ and $n = 6$ to lower levels. Only a few semiempirical wavelengths of $n = 5$ levels have been reported by Seely et al. [14]. For the $5d\,^2D_{5/2}$–$4p\,^2P_{3/2}$ transition, the wavelengths between the present value (λ = 9.477 Å) and the semiempirical value reported by Seely et al. [14] (λ = 9.487 Å) are in good agreement with a relative difference of 0.10%. Similarly for $5f\,^2F_{5/2}$–$4d\,^2D_{3/2}$, $5f\,^2F_{7/2}$–$4d\,^2D_{5/2}$, $5g\,^2G_{7/2}$–$4f\,^2\mathrm{F}_{5/2}$, and $5g\,^2G_{9/2}$–$4f\,^2F_{7/2}$ transitions, the present wavelengths are 9.864, 10.076, 10.361, 10.448 Å and the semiempirical values are 9.872, 10.075, 10.357, 10.443 Å, as respectively reported by Seely et al. [14]. The relative differences between these wavelengths are 0.08, 0.00, 0.03, and 0.04%, respectively.

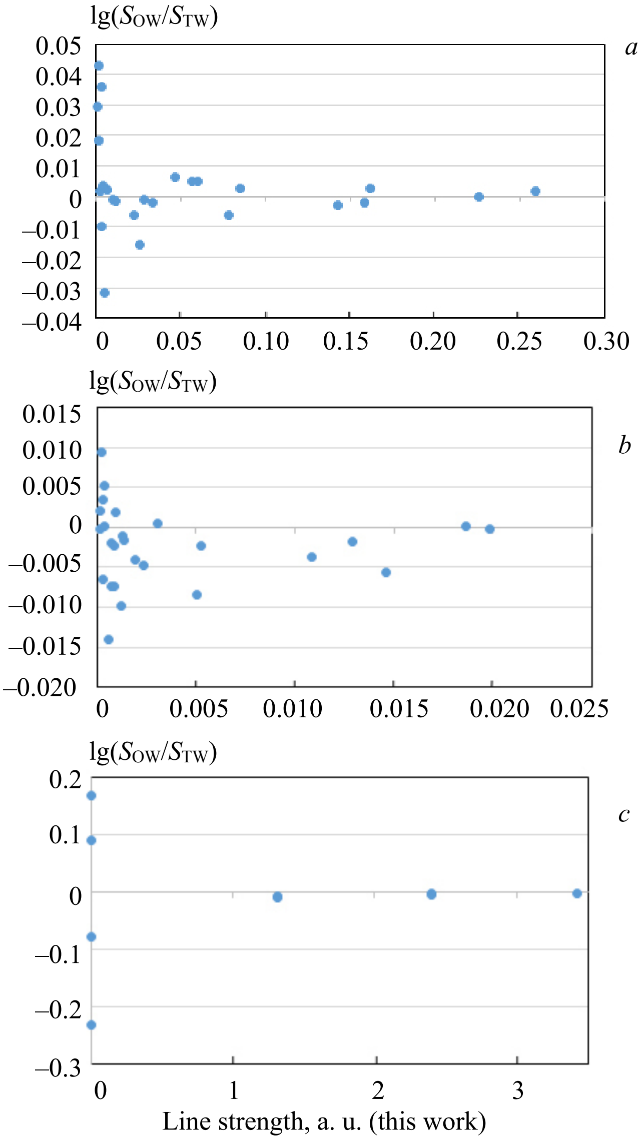

Fig. 2. The relation of the line strengths values between this work (S_{TW}) and the other works (S_{OW}) [14] for E1 transitions (a) and for E2 transitions (b), and this work (S_{TW}) for M1 transitions (c).

TABLE 2. Transition probabilities, A_{ij} (s^{-1}), line strengths, S (a. u.), and wavelengths, λ (Å), among states with principal quantum numbers n = 3 and n = 4 for E1 transitions in Hf^{61+}. Numbers in brackets represent powers of 10. We have omitted the core $1s^2 2s^2 2p^6$ in this table

Transitions				A_{ij}, s^{-1}		S, a. u.		λ, Å	
Upper level		Lower level		This work	Other works	This work	Other works	This work	Other works
3p	$^2P_{1/2}$	3s	$^2S_{1/2}$	4.06[10]	4.057[10][b] 4.044[10][c]	2.198[-02]	2.167[-02][c]	81.844	81.082[a] 81.053[d]
3p	$^2P_{3/2}$	3s	$^2S_{1/2}$	1.36[12]	1.365[12][b] 1.376[12][c]	4.614[-02]	4.680[-02][c]	25.789	25.769[a] 25.760[d]
3d	$^2D_{3/2}$	3p	$^2P_{1/2}$	1.16[12]	1.149[12][c]	3.294[-02]	3.279[-02][c]	24.292	24.336[d]
3d	$^2D_{3/2}$	3p	$^2P_{3/2}$	1.02[10]	1.019[10][c]	6.451[-03]	6.480[-03][c]	68.453	–
3d	$^2D_{5/2}$	3p	$^2P_{3/2}$	1.84[11]	1.794[11][c]	5.983[-02]	6.048[-02][c]	47.933	48.424[d]
4s	$^2S_{1/2}$	3p	$^2P_{1/2}$	1.43[13]	1.501[13][b] 1.448[13][c]	1.082[-03]	1.129[-03][c]	4.247	–
4s	$^2S_{1/2}$	3p	$^2P_{3/2}$	4.65[13]	4.248[13][b] 4.179[13][c]	5.033[-03]	4.678[-03][c]	4.788	4.838[d]
4p	$^2P_{1/2}$	3s	$^2S_{1/2}$	5.06[13]	5.367[13][c]	3.107[-03]	3.375[-03][c]	3.961	3.992[d]
4p	$^2P_{1/2}$	3d	$^2D_{3/2}$	1.32[13]	1.410[13][c]	1.647[-03]	1.818[-03][c]	5.023	–
4p	$^2P_{1/2}$	4s	$^2S_{1/2}$	8.79[09]	1.011[10][c]	7.831[-02]	7.719[-02][c]	208.201	–
4p	$^2P_{3/2}$	3s	$^2S_{1/2}$	3.47[13]	3.396[13][c]	3.740[-03]	3.762[-03][c]	3.794	3.825[d]
4p	$^2P_{3/2}$	3d	$^2D_{3/2}$	7.85[11]	8.136[11][c]	1.670[-04]	1.787[-04][c]	4.758	–
4p	$^2P_{3/2}$	3d	$^2D_{5/2}$	8.65[12]	8.424[12][c]	2.015[-03]	2.022[-03][c]	4.904	–
4p	$^2\mathrm{P}_{3/2}$	4s	$^2S_{1/2}$	3.28[11]	3.294[11][c]	1.611[-01]	1.620[-01][c]	62.907	–
4d	$^2D_{3/2}$	3p	$^2P_{1/2}$	8.30[13]	8.041[13][c]	9.662[-03]	9.633[-03][c]	3.893	3.929[d]
4d	$^2D_{3/2}$	3p	$^2P_{3/2}$	1.91[13]	1.808[13][c]	3.081[-03]	3.011[-03][c]	4.341	–
4d	$^2D_{3/2}$	4p	$^2P_{1/2}$	3.33[11]	3.132[11][c]	1.419[-01]	1.410[-01][c]	59.997	–
4d	$^2D_{3/2}$	4p	$^2P_{3/2}$	2.48[09]	2.419[09][c]	2.822[-02]	2.816[-02][c]	179.404	–
4d	$^2D_{5/2}$	3p	$^2P_{3/2}$	1.10[14]	1.030[14][c]	2.580[-02]	2.487[-02][c]	4.290	4.334[d]
4d	$^2D_{5/2}$	4p	$^2P_{3/2}$	5.01[10]	4.746[10][c]	2.588[-01]	2.598[-01][c]	120.413	–
4f	$^2F_{5/2}$	3d	$^2D_{3/2}$	2.07[14]	2.020[14][c]	5.635[-02]	5.701[-02][c]	4.517	4.564[d]
4f	$^2F_{5/2}$	3d	$^2D_{5/2}$	1.43[13]	1.395[13][c]	4.246[-03]	4.281[-03][c]	4.648	–
4f	$^2F_{5/2}$	4d	$^2D_{3/2}$	9.68[09]	8.934[09][c]	1.583[-01]	1.576[-01][c]	176.806	–
4f	$^2F_{5/2}$	4d	$^2D_{5/2}$	9.42[07]	9.170[07]	1.114[-02]	1.110[-02][c]	341.864	–
4f	$^2F_{7/2}$	3d	$^2D_{5/2}$	2.16[14]	2.109[14][c]	8.437[-02]	8.490[-02][c]	4.623	4.667[d]
4f	$^2F_{7/2}$	4d	$^2D_{5/2}$	3.90[09]	3.796[09][c]	2.259[-01]	2.258[-01][c]	244.769	–

[a,b,c,d] Ref. [17, 11, 12, 14], respectively.

TABLE 3. Transition probabilities, A_{ij} (s^{-1}), line strengths, S (a. u.), and wavelengths, λ (Å), among states with principal quantum numbers n = 3 and n = 4 for E2 and M1 transitions in Hf^{61+}. Numbers in brackets represent powers of 10. We have omitted the core $1s^2 2s^2 2p^6$ in this table

Transitions					A_{ij}, s^{-1}		S, a. u.		λ, Å
Upper level		Lower level		Transition type	This work	Ref. [12]	This work	Ref. [12]	This work
3p	$^2P_{3/2}$	3p	$^2P_{1/2}$	E2	4.44[06]	4.26[06]	1.199[-03]	1.172[-03]	37.650
				M1	1.67[08]	1.61[08]	1.318[00]	1.293[00]	
3d	$^2D_{3/2}$	3s	$^2S_{1/2}$	E2	1.05[08]	1.03[08]	8.605[-04]	8.559[-04]	18.730
3d	$^2D_{5/2}$	3s	$^2S_{1/2}$	E2	1.90[08]	1.84[08]	1.346[-03]	1.341[-03]	16.770
3d	$^2D_{5/2}$	3d	$^2D_{3/2}$	E2	5.61[02]	4.65[02]	3.138[-04]	3.091[-04]	159.900
				M1	2.64[06]	2.35[06]	2.399[00]	2.368[00]	
4s	$^2S_{1/2}$	3d	$^2D_{3/2}$	E2	3.23[10]	3.11[10]	2.082[-04]	2.128[-04]	5.150
4s	$^2S_{1/2}$	3d	$^2D_{5/2}$	E2	4.81[10]	4.55[10]	3.656[-04]	3.658[-04]	5.320
4p	$^2P_{1/2}$	3p	$^2P_{3/2}$	E2	1.86[11]	1.73[11]	7.437[-04]	7.311[-04]	4.680
				M1	9.71[08]	1.16[09]	7.382[-03]	9.109[-03]	

Continue Table 3

Transitions					A_{ij}, s^{-1}		S, a. u.		λ, Å
Upper level		Lower level		Transition type	This work	Ref. [12]	This work	Ref. [12]	This work
4*p*	$^2P_{3/2}$	3*p*	$^2P_{1/2}$	E2	9.37[10]	9.01[10]	3.338[-04]	3.365[-04]	8.90[-04]
				M1	6.76[08]	5.48[08]	6.313[-03]	5.271[-03]	
4*p*	$^2P_{3/2}$	3*p*	$^2P_{3/2}$	E2	9.29[10]	8.54[10]	5.784[-04]	5.601[-04]	4.450
4*p*	$^2P_{3/2}$	4*p*	$^2P_{1/2}$	E2	6.86[05]	6.01[05]	1.459[-02]	1.440[-02]	90.140
				M1	1.21[07]	1.11[07]	1.318[00]	1.300[00]	
4*d*	$^2D_{3/2}$	3*s*	$^2S_{1/2}$	E2	3.67[11]	3.52[11]	9.282[-04]	9.322[-04]	3.720
4*d*	$^2D_{3/2}$	3*d*	$^2D_{3/2}$	E2	5.22[10]	5.00[10]	3.987[-04]	4.036[-04]	4.640
4*d*	$^2D_{3/2}$	3*d*	$^2D_{5/2}$	E2	2.18[10]	2.07[10]	1.934[-04]	1.933[-04]	4.770
				M1	4.35[07]	6.22[07]	7.010[-04]	1.035[-03]	
4*d*	$^2D_{3/2}$	4*s*	$^2S_{1/2}$	E2	1.64[07]	1.62[07]	1.287[-02]	1.282[-02]	46.580
4*d*	$^2D_{5/2}$	3*s*	$^2S_{1/2}$	E2	3.68[11]	3.50[11]	1.326[-03]	1.323[-03]	3.680
4*d*	$^2D_{5/2}$	3*d*	$^2D_{3/2}$	E2	1.50[10]	1.42[10]	1.612[-04]	1.620[-04]	4.580
				M1	3.22[07]	1.82[07]	6.871[-04]	4.035[-04]	
4*d*	$^2D_{5/2}$	3*d*	$^2D_{5/2}$	E2	5.87[10]	5.54[10]	7.301[-04]	7.267[-04]	4.710
4*d*	$^2D_{5/2}$	4*s*	$^2S_{1/2}$	E2	3.07[07]	2.96[07]	1.980[-02]	1.979[-02]	41.320
4*d*	$^2D_{5/2}$	4*d*	$^2D_{3/2}$	E2	1.49[02]	1.18[02]	5.239[-03]	5.211[-03]	366.200
				M1	2.20[05]	1.91[05]	2.398[00]	2.381[00]	
4*f*	$^2F_{5/2}$	3*p*	$^2P_{1/2}$	E2	5.44[11]	5.12[11]	2.335[-03]	2.31[-03]	3.810
4*f*	$^2F_{5/2}$	3*p*	$^2P_{3/2}$	E2	1.15[11]	1.06[11]	8.377[-04]	8.237[-04]	4.240
4*f*	$^2F_{5/2}$	4*p*	$^2P_{1/2}$	E2	1.12[07]	1.00[07]	1.082[-02]	1.073[-02]	44.800
4*f*	$^2F_{5/2}$	4*p*	$^2P_{3/2}$	E2	1.01[05]	9.36[04]	3.042[-03]	3.046[-03]	89.050
4*f*	$^2F_{7/2}$	3*p*	$^2P_{3/2}$	E2	5.27[11]	4.90[11]	5.017[-03]	4.92[-03]	4.220
4*f*	$^2F_{7/2}$	4*p*	$^2P_{3/2}$	E2	7.63[05]	7.05[05]	1.866[-02]	1.867[-02]	80.710
4*f*	$^2F_{7/2}$	4*f*	$^2F_{5/2}$	E2	5.66[-01]	5.28[-01]	1.923[-03]	1.905[-03]	861.810
				M1	1.81[04]	1.73[04]	3.428[00]	3.405[00]	

Theoretical spectroscopic parameters for E2 and M1 transitions presented in [12] compared to the lines are listed in Table 3. The available data for the excited configurations of these forbidden transitions are very limited. The plot of ratios of the two calculations (S_{OW}/S_{TW}) against the line strength from our calculations (S_{TW}) for E2 and M1 transitions are shown in Figs. 2b,c. It can be inferred that the wavelengths, transition probabilities, and line strengths are quite close to the theoretical data of the other works [12].

Conclusions. Energy levels, wavelengths, transition probabilities and line strengths for E1, E2, and M1 transitions in Na-like Hf LXII are reported. Energy levels and transition parameters produced using AUTOSTRUCTURE are in good agreement compared to the data in the literature. This study provides a new accurate set of spectroscopic data for highly charged heavy elements which are significant for magnetic and intertial confinement fusion research. We hope that the results will provide guidance and facilitate future experiments.

REFERENCES

1. C. Biedermann, R. Radtke, R. Seidel, T. Pütterich, *Phys. Scr.*, **134**, 014026(1–6) (2009).
2. S. Hamasha, R. Alshaiub, *Phys. Scr*., **86**, 065302(1–14) (2012).
3. K. Blagoev, P. Bogdanovich, N. Dimitrov, A. Momkauskaite, *Phys. Rev. A*, **37**, 4679–4684 (1988).
4. G. G. Konan, L. Ozdemir. *Chin. J. Phys*., **54**, 433–450 (2016).
5. G. G. Konan, L. Ozdemir, G. Urer, *J. Quant. Spectrosc. Radiat. Transfer*, **145**, 110–120 (2014).
6. G. G. Konan, *Can. J. Phys*., **97**, 959–965 (2019).
7. G. G. Konan, L. Özdemir, *Can. J. Phys.,* **96**, 1098–1103 (2018).
8. M. R. Gilbert, J. Ch. Sublet, *Nucl. Fusion*, **51**, 043005(1–8) (2011).
9. A. Kramida, Yu. Ralchenko, J. Reader, NIST ASD Team, NIST Atomic Spectra Database (version 5.2), [Online]. Available: Wednesday, 03-Sep-2022, https://www.nist.gov/pml/atomic-spectra-database.
10. R. J. Hawryluk, D. J. Campbell, G. Janeschitz, P. R. Thomas, et al., *Nucl. Fusion*, **49**, 065012(1–3) (2009).

11. W. R. Johnson, Z. W. Liu, J. Sapirstein, *At. Data Nucl. Data Tables*, **64**, 279–300 (1996).
12. D. H. Baik, Y. G. Ohr, K. S. Kim, J. M. Lee, P. Indelicato, Y. K. Kim, *At. Data Nucl. Data Tables*, **47**, 177–203 (1991).
13. Y. K. Kim, D. H. Baik, P. Indelicato, J. P. Desclaux, *Phys. Rev. A*, **44**, 148–166 (1991).
14. J. F. Seely, C. M. Brown, U. Feldman, J. O. Ekberg, C. J. Keane, B. J. Macgowan, D. R. Kania, W. E. Behring, *At. Data Nucl. Data Tables*, **47**, 1–15 (1991).
15. D. H. Sampson, H. L. Zhang, C. J. Fontes, *At. Data Nucl. Data Tables*, **44**, 209–271 (1990).
16. L. N. Ivanov, E. P. Ivanova, *At. Data Nucl. Data Tables*, **24**, No. 2, 95–109 (1979).
17. J. D. Gillaspy, I. N. Draganic, Yu. Ralchenko, J. Reader, J. N. Tan, J. M. Pomeroy, S. M. Brewer, *Phys. Rev. A*, **80**, 010501(1–3) (2009).
18. J. D. Gillaspy, D. Osin, Y. Ralchenko, J. Reader, S. A. Blundell, *Phys. Rev. A*, **87**, 062503(1–10) (2013).
19. J. Sapirstein, K. T. Cheng, *Phys. Rev. A*, **91**, 062508(1–9) (2015).
20. C. J. Fontes, H. L. Zhang, *At. Data Nucl. Data Tables*, **113**, 293–315 (2017).
21. N. R. Badnell, *Comp. Phys. Commun.*, **182**, 1528–1535 (2011).
22. N. R. Badnell, *J. Phys. B*, **19**, 3827–3835 (1986).
23. N. R. Badnell, *J. Phys. B*, **30**, 1–11 (1997).